Strojniški vestnik - Journal of Mechanical Engineering 56(2010)5, 307-315 Paper received: 09.10.2008
UDC 532.5:519.876.5 Paper accepted: 15.02.2010

Application of Non-Discrete Boundaries with Friction to Smoothed Particle Hydrodynamics

Gregor Petkovšek[1,2*] - Elvira Džebo[1] - Matjaž Četina[1] - Dušan Žagar[1]
[1]University of Ljubljana, Faculty of Civil and Geodetic Engineering, Slovenia
[2]CGS plus d.o.o., Slovenia

Smoothed particle hydrodynamics (SPH) is a meshless particle method for simulation of fluid flows. It is especially suitable for simulating flows with rapid changes. Treating the solid boundaries, however, is not as straightforward as with finite element or finite volume based methods. This paper describes a non-discrete boundary with friction approach to model particle-boundary interaction. This approach is mathematically consistent with the solution for the particle-particle interaction, and it provides a continuous solution along the boundary. The proposed model was verified against the experiments of Martin & Moyce [1] and numerical simulations by other authors. The results showed at least as good overall agreement as the simulations of other models, while local behaviour at the boundaries was better.

Keywords: hydrodynamic simulation, meshless particle method, boundary treatment, fluid column collapse

0 INTRODUCTION

For simulations in fluid dynamics, approaches based on Eulerian principles are usually used, such as finite difference, finite volume, or finite element methods. These methods can be applied to a wide range of hydrodynamic problems and enable simulations with reasonable computational times. However, despite their popularity and a wide range of applicability, these methods also have certain disadvantages. Due to the Eulerian description of flow, convective terms appear in the equations of motion, which may result in numerical diffusion. If a fixed mesh is used, it has to be refined in points of interesting flow features. When these locations change with time or are not known in advance, a fine numerical mesh must be constructed all over the domain in which case the simulation becomes computationally expensive. These problems can partially be avoided by attaching numerical mesh to fluid particles (Lagrangian principle). However, in cases of complex flow (e.g. rotational flow), the particle-based numerical mesh becomes too distorted.

When these types of problems arise, the SPH, a mesh free Lagrangian numerical technique for simulation in fluid dynamics, can be applied. It was developed by Lucy [2] and Gingold & Monaghan [3] and initially used to study problems in astrophysics. As the method proved able to treat large deformations and rapid changes in flow patterns, it was later adapted for solving problems of dynamic material strength [4], free surface flow [5], explosions [6], and similarly. Free surface flows applications include dam break analysis [7] and [8], wave-structure interaction [9], non-Newtonian flows [10] and [12] and multi-phase flows [13] and [14].

When adapting the method to free surface flows, fluid compressibility is an important issue. Monaghan [5] treated water as a weakly compressible fluid whose compressibility is dependant on the maximum expected fluid velocity rather than true sound velocity of water. This was necessary for practical reasons, as the time step depends on the velocity of sound.

Another issue specific to free surface flows is the boundary conditions. Solid boundary conditions are usually satisfied by the use of boundary particles. A review is given in Crespo et al. [15]. Ghost particles [16] are constructed at each time step so that the particles near the boundary are mirrored across the boundary face. Monaghan [5] proposed repulsive particles that exert a normal force to particles approaching the

*Corr. Author's Address: CGS plus d.o.o., Brnčičeva 13, SI-1000 Ljubljana, Slovenia, gregor.petkovsek@cgsplus.si

boundary. The force depends on the distance between the particle and a boundary and the velocity of the particle, perpendicular to the boundary. Darlymple & Knio [17] presented the dynamic particles that follow the same equations of continuity and state, but their position is prescribed externally. Marongiu et al. [18] proposed a new type of boundary particles that are mathematically consistent with the SPH formulation.

Monaghan & Kos [19] found that if boundaries are made of particles that exert a central force, they produce the equivalent of a corrugated boundary with ripples on the scale of the particle spacing. The proposed solution was to implement an interpolation procedure so that the forces from neighbouring boundary particles produce a force that is constant and normal to the boundary.

For a slightly different set of equations than presented in this paper, an innovative method to handle contact forces between particles and rigid solid boundaries, based on the variational approach, was introduced by Kulasegaram et al [20]. They studied several boundary shapes and proposed a correction factor for use within their basic 2D equations. A similar approach was used by Bonet et al. [21].

In this paper, we propose a method that is both consistent as in Marongiu et al. [18] and removes the ripples effect as in Monaghan and Kos [19]. The method is strictly valid only for flat boundaries, but is simple to implement and can be used in 3D cases. In addition, we investigate the effect of boundary friction on flow patterns by allowing a different value of friction coefficient for boundaries.

1 METHOD

In SPH, the interpolation of a value A anywhere in the computational domain is performed by means of the smoothing kernel W as in Monaghan [22]:

$$A(\mathrm{r}_\mathrm{i}) \approx \int A(\mathrm{r}) W(\mathrm{r}-\mathrm{r}_\mathrm{i}) d\,\mathrm{r} \,. \tag{1}$$

The integral is taken over D, the domain of influence of W. In discrete form, it can be expressed as:

$$A(\boldsymbol{r_i}) = \sum\nolimits_j \frac{m_j}{\rho_j} A_j W(\boldsymbol{r_j}-\boldsymbol{r_i}) \,, \tag{2}$$

where m_j is the mass of the particle j, ρ_j is its density and A_j the value of A at the location of particle j. Smoothing kernels can have different forms. In this paper, we use the cubic spline proposed by Monaghan & Lattanzio [23]

$$W(q) = \frac{1}{w}\begin{cases} 1-\frac{3}{2}q^2+\frac{3}{4}q^3 & 0 \le q < 1 \\ \frac{1}{4}(2-q)^3 & 1 \le q < 2 \\ 0 & 2 < q \end{cases}, \tag{3}$$

where $q = l/h$, l is the distance between particles and h is the kernel smoothing length. w is a normalization factor, and is equal to $7\pi h^2/10$ for two-dimensional simulations and πh^3 for three-dimensional simulations. For simulations described in this paper, the length of smoothing kernel was taken to be $h = 1.2\ d_0$, where d_0 is the initial particle spacing.

The main advantage of SPH becomes evident when computing gradients of a function A. It can be replaced by computing the gradient of smoothing kernel instead, which is a straightforward operation. This is achieved by integrating by parts

$$\begin{aligned} \nabla A(\mathrm{r}_\mathrm{i}) &\approx \int \nabla A(\mathrm{r}) W(\mathrm{r}-\mathrm{r}_\mathrm{i}) d\,\mathrm{r} = \\ &= \int A(\mathrm{r}) W(\mathrm{r}-\mathrm{r}_\mathrm{i}) d\,\mathrm{S} - \int A(\mathrm{r}) \nabla W(\mathrm{r}-\mathrm{r}_\mathrm{i}) d\,\mathrm{r} \end{aligned}, \tag{4}$$

The first term on the right-hand side of the bottom line is the integral over the boundary of D and $d\boldsymbol{S}$ is normal to the boundary. It equals zero everywhere inside the fluid domain, because W is zero when r'-$r \ge 2h$. In the standard SPH formulation, the impact of the boundaries on the particles is achieved through the repulsive forces of the boundary particles, therefore the value of this term is always taken to be zero. In this paper, we propose the impact of the boundaries to be computed through this term, as shown later.

The governing equations consist of dynamic and continuity equations and the equation of state. In their continuous form, they are expressed as follows:

$$\frac{d\boldsymbol{v}}{dt} = -\frac{1}{\rho}\nabla P + \upsilon \Delta \boldsymbol{v} + \frac{\upsilon}{3}\nabla(\nabla \boldsymbol{v}) + \boldsymbol{g} \,, \tag{5}$$

$$\frac{d\rho}{dt} = -\rho \nabla \boldsymbol{v} \ , \tag{6}$$

$$P = c^2(\rho - \rho_0) \ , \tag{7}$$

where velocity vector is denoted by $\boldsymbol{v}$, P is pressure, υ kinematic viscosity and g is gravity acceleration. The artificial speed of sound c is taken as 10-times the maximum expected velocity.

After applying the SPH interpolation rules and making expressions symmetric (e.g. Monaghan [22]), the Eqs. (5) and (6) are transformed to

$$\frac{d\boldsymbol{v}_i}{dt} = \sum_j \left(\left(-\left(\frac{p_i}{\rho_i^2} + \frac{p_j}{\rho_j^2} \right) + \frac{\upsilon'}{3} \frac{\boldsymbol{v}_{ij}\boldsymbol{r}_{ij}}{\boldsymbol{r}_{ij}\boldsymbol{r}_{ij}} \right) \boldsymbol{e}_{ij} + \frac{\upsilon' \boldsymbol{v}_{ij}}{|\boldsymbol{r}_{ij}|} \right) m_j W'_{ij} + \boldsymbol{g} \ , \tag{8}$$

$$\frac{d\rho_i}{dt} = \sum_j \boldsymbol{v}_{ij}\, \boldsymbol{e}_{ij}\, m_j W'_{ij} \ , \tag{9}$$

notation A_{ij} is used instead of A_i-A_j for any quantity A. W_{ij}' is a derivative of W with respect to l (the distance between points). υ' is kinematic viscosity υ (see Eq. 10) divided by the average density of particles i and j.

The kinematic viscosity υ can be approximated for turbulent flow as

$$\upsilon = a' d_0^2 \frac{|\boldsymbol{v}_{ij}|}{l} = ah^2 \frac{|\boldsymbol{v}_{ij}|}{l} \ , \tag{10}$$

where a' = 0.12^2 = 0.0144 [9] or a = 0.01 for the particle interactions.

In this study, the particle-boundary interactions are computed as a product of the surface integral of the kernel value over the kernel-solid boundary contact surface and estimated constant values of physical quantities on the boundary, instead of using summation over boundary particles. The value of the surface integral

$$WI = \int W(\mathrm{r} - \mathrm{r_i}) d\mathrm{S} \tag{11}$$

in terms of q for flat surfaces for a 3D case is

$$WI(q) = \frac{1}{h} \begin{cases} 0.7 - q^2\left(1 - \frac{3}{4}q^2 + \frac{3}{10}q^3\right) & 0 \le q < 1 \\ 0.8 - q^2\left(2 - 2q + \frac{3}{4}q^2 - \frac{1}{10}q^3\right) & 1 \le q < 2 \\ 0 & 2 < q \end{cases} . \tag{12}$$

Schematics of the integration over a flat surface are shown in Fig. 1. For curved surfaces, this solution must only be treated as an approximation.

The velocity on the boundary is prescribed (zero for solid still boundary) and boundary pressure is calculated as

$$P_b = \max(0; P_i; cv_p / l) \, , \tag{13}$$

where P_i, ρ_i and v_p are the pressure, density and velocity perpendicular and relative to the boundary of the particle that interacts with the boundary. The term cv_p/l prevents the particles from penetrating the boundary, and is only taken into account for particles approaching the boundary (e.g. Monaghan & Kos [19]).

The equations for particle-boundary interaction thus become:

$$\frac{d\boldsymbol{v}_{i,b}}{dt} = \left(\left(\frac{P_b + P_i}{\rho_i} - \frac{\upsilon_b}{3} \frac{\boldsymbol{v}_{ib}\boldsymbol{e}_{ib}}{l} \right) \boldsymbol{e}_n - \frac{\upsilon_b \boldsymbol{v}_{ib}}{l} \right) WI \ , \tag{14}$$

$$\frac{d\rho_{i,b}}{dt} = \rho_i \, \boldsymbol{v}_{ib} \boldsymbol{e}_{ib} \, WI \ . \tag{15}$$

Normal to the boundary is denoted by $\boldsymbol{e_n}$, while υ_b is the "boundary" viscosity, calculated from Eq. 10, except that instead of a fixed value of a, a value appropriate to boundary sub scale roughness b is used.

For particles within reach of the boundary, the Eqs. (14) and (15) are added to the discrete governing Eqs. (8) and (9).

To prevent oscillations of pressure field, several techniques have been proposed. In this paper, we follow the approach of Molteni & Colagrossi [24], where additional density flux ρ_F between particles i and j is applied:

$$\rho_F = 0.4 \cdot c \cdot h \cdot \frac{\rho_{ij}}{|\mathrm{r_{ij}}|} \cdot d_0^3 \cdot W'_{ij} \ . \tag{16}$$

The density flux is added to Eq. (9). Verlet algorithm [25] was used for time stepping.

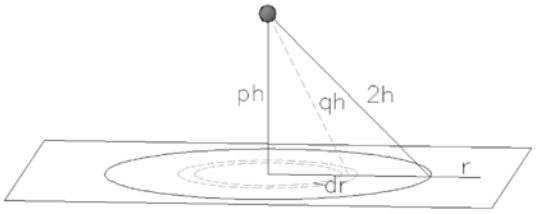

Fig. 1. *Integration of kernel over a flat surface*

2 NUMERICAL EXPERIMENTS

The simulations of the developed model (Tis Isat) were compared to measurements of the collapse of a two-dimensional rectangular fluid column, as described in Martin & Moyce [1]. Three different heights of fluid columns were used, the ratios between height (H_0) and width (W_0) of the fluid column were 1, 2 and 4.

The results of the model were also compared to the results of the free open-source SPH code SPHYSICS [26]. Comparisons of dimensionless surge front distance from the initial position and the relative residual height of the fluid column were performed.

Several authors [5], [7] and [28] achieved acceptable agreement of models and numerical results of the mentioned experiment close to the initial time, while larger discrepancies occurred further downstream. Therefore, special attention in the simulations performed with the Tis Isat model was paid to propagation of the collapsing fluid column through longer time intervals. The correct information on propagation of surge front and particularly on the fluid height at a certain downstream location can be of practical importance in dam-break simulations.

The parameters used for the initial experiment with the Tis Isat model are given in Table 1. Some of the parameters were further varied in order to determine the sensitivity of the new model to these parameters. The parameters chosen for the SPHYSICS model are listed in Table 2. Although not the same, the closest possible parameters for both models were chosen. With the SPHYSICS model, two different boundary conditions, the dynamic [17] and the repulsive boundary condition [19] were tested at the solid wall. Furthermore, two different algorithms were used for time stepping: Verlet [25] and Predictor – corrector [29].

3 RESULTS AND DISCUSSION

The comparisons of measurements [1] and the results of the initial simulation with the Tis Isat model, as well as with the SPHYSICS model are shown in Figs. 2 to 4, for water columns with the initial height / width ratio of the fluid column 1, 2, and 4, respectively. The values in the figures are normalised to the initial width (W_0) or height (H_0) of the fluid column at the ordinate axis and the time at the abscise axis is normalised as proposed by Martin & Moyce [1]:

$$T = nt\sqrt{\boldsymbol{g}/W_0}\ , \tag{17}$$

where n^2 denotes the H_0/W_0 ratio, t is the model / experiment time, g is the gravity acceleration and W_0 is the semi-base length (dimensional characteristic of the column base).

The results of the Tis Isat model show slightly faster propagation of the surge front than measured, while the height of the fluid column decreases accurately. A comparison of the results of the new code and the SPHYSICS model shows that using the non-discrete boundaries with friction results in at least the same level of agreement with measurements.

Table 1. *Initial parameters of the numerical experiment performed with the Tis Isat model*

Parameter	Abbreviation	Value
Number of particles	*np*	2500 (50 x 50); 5000 (50 x 100); 10000 (50 x 200)
Initial particle distance	*lo*	0.001143 m
Coefficient (to calculate eddy viscosity within fluid)	*a*	0.01
Coefficient (to calculate eddy viscosity on the walls)	*b*	0.01

Table 2. *Initial parameters used with the SPHYSICS model*

Parameter	Abbreviation	Value
Number of particles	*np*	2500 (50 x 50); 5000 (50 x 100); 10000 (50 x 200)
Particle distance	*l*o	0.001143 m
Viscosity	*i*_viscos	Laminar + SPS
Reinitialisation	--	Shepard filter / MLS

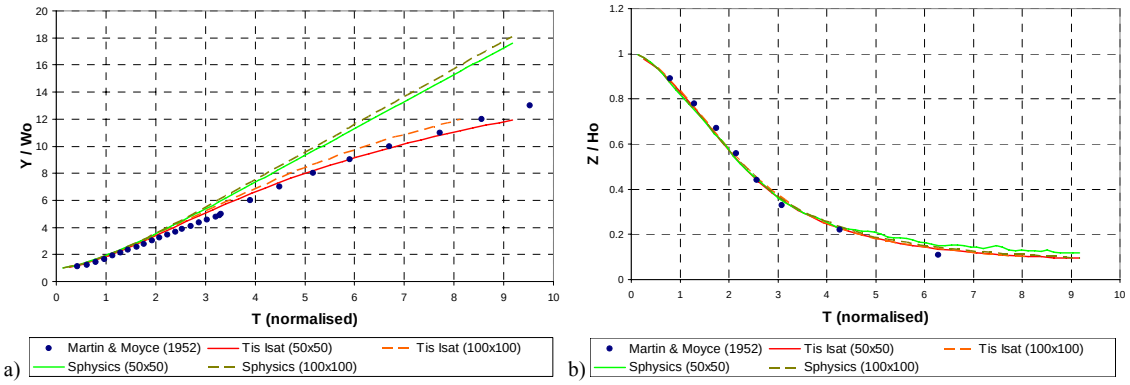

Fig. 2. *Comparison of surge front propagation and relative height of the fluid column; $H_0/W_0 = 1$*
a) Surge front propagation; b) Relative height of the water column

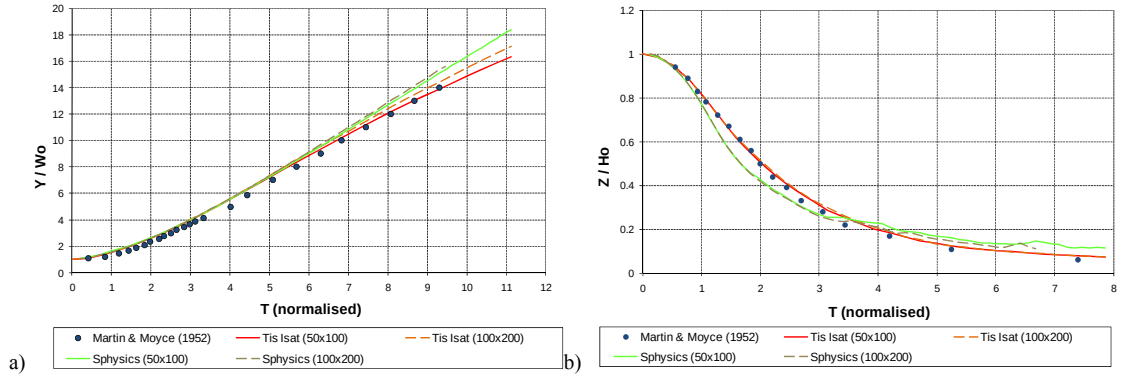

Fig. 3. *Comparison of surge front propagation and relative height of the fluid column; $H_0/W_0 = 2$*
a) Surge front propagation; b) Relative height of the water column

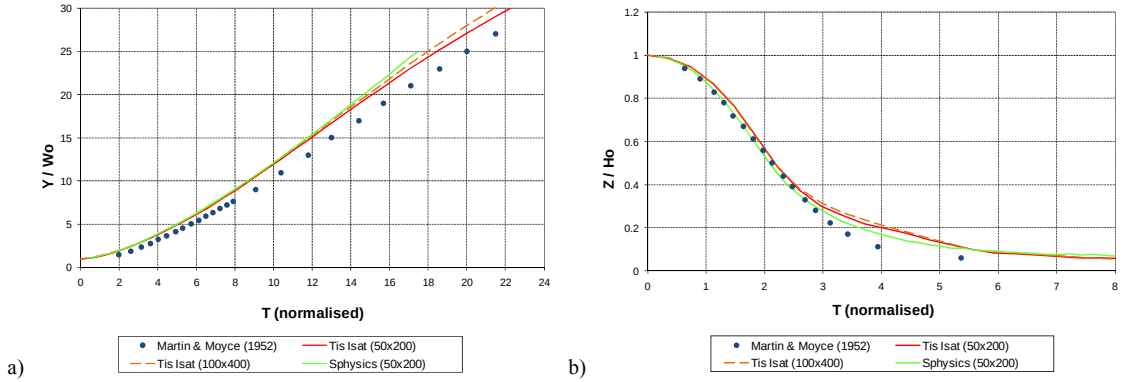

Fig. 4. *Comparison of surge front propagation and relative height of the fluid column; $H_0/W_0 = 4$*
a) Surge front propagation; b) Relative height of the water column

A similar level of agreement can be observed with the results of other authors using their own models and performing the same experiment (e.g. [5], [7], [27] and [28]).

In the third case (Fig. 4), the poorer agreement in the maximum relative height graph at the normalised time $T>3$ is due to the increased fluid level in the middle of the channel, while all measurements were performed at the upstream boundary. Using the SPHYSICS model, some particles stayed stuck to the solid wall (Fig. 7); therefore, a distance of 3 particle diameters was

excluded from the observation of the maximum relative height in these simulations.

The comparison of fluid propagation shows some disturbances in simulations with the SPHYSICS code. At the upstream boundary, particles are shifted away from the wall (Fig. 5). This phenomenon, which stems from the definition of the upstream boundary condition has been noticed by Monaghan [5], and has no physical background. It further results in a disturbance of the surface of the collapsing fluid column (Fig. 6).

Moreover, SPHYSICS simulations with a smaller number of particles show that a number of particle groups secede at the surge front while some particles stay stuck to the wall (Fig. 7). Using the non-discrete boundary condition with friction eliminates such disturbances in the collapsing fluid column at the rigid wall as well as at the surge front.

In order to determine the sensitivity of the new code to different input parameters, several further simulations were performed. Fig. 8 shows the behaviour of the collapsing fluid column represented by a different total number of particles. As expected, smaller numbers resulted in more friction and slower propagation of the surge front while the propagation was faster using larger numbers of particles. The Tis Isat model also showed higher sensitivity to the variability of the wall viscosity coefficient (Fig. 9), while the dependence of results on all other parameters was significantly lower.

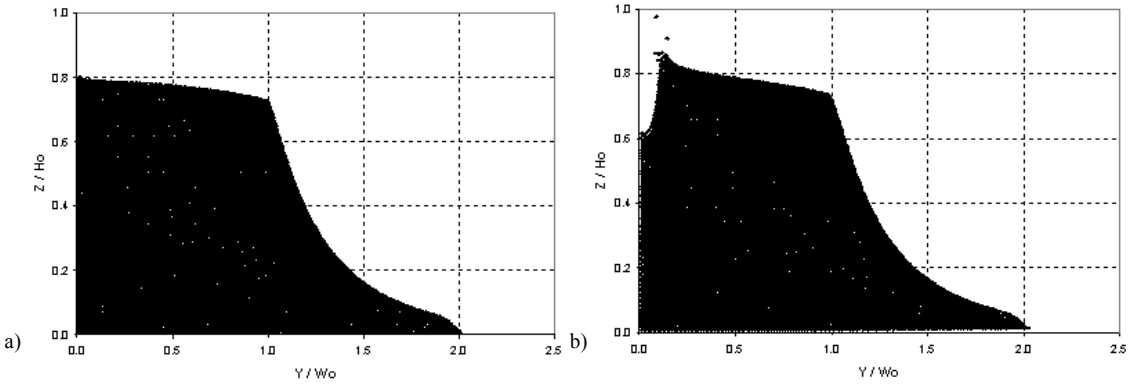

Fig. 5. *Comparison of fluid propagation, 50 x 100 particles after 0.08 s, a) the Tis Isat model, b) the SPHYSICS model*

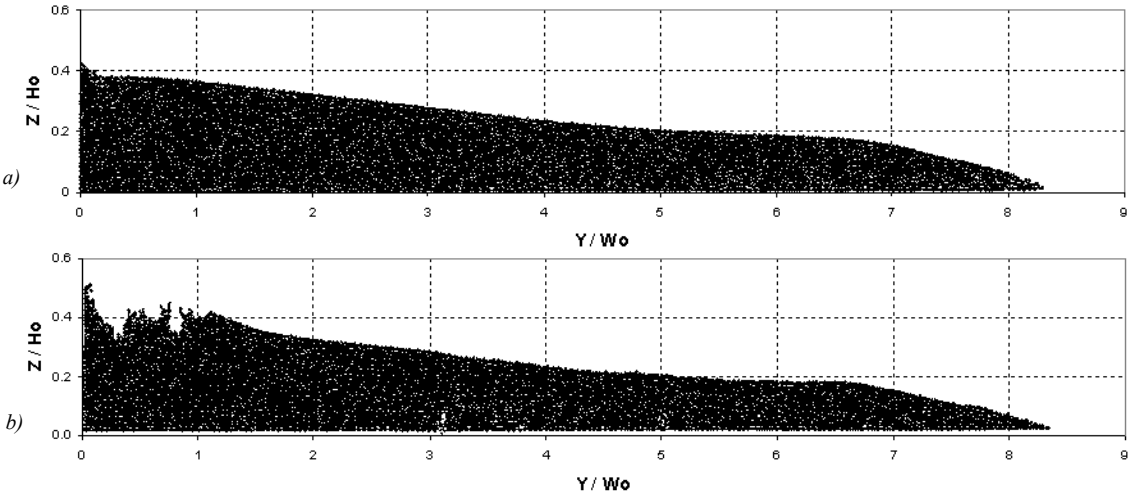

Fig. 6. *Comparison of fluid propagation, 50 x 100 particles after 0.3 s, a) the Tis Isat model, b) the SPHYSICS model*

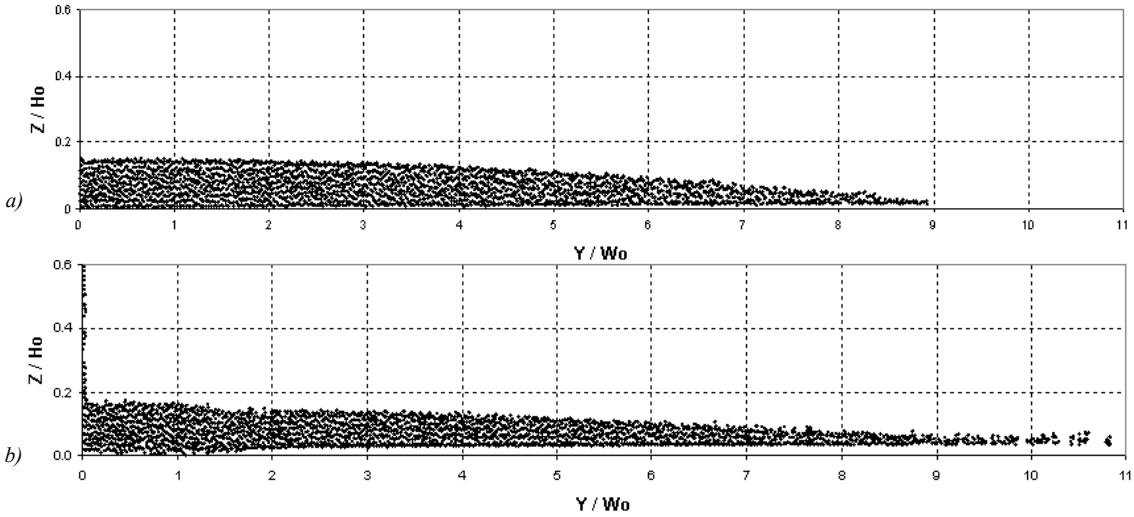

Fig. 7. *Comparison of fluid propagation, 50 x 50 particles after 0.44 s, a) the Tis Isat model, b) the SPHYSICS model*

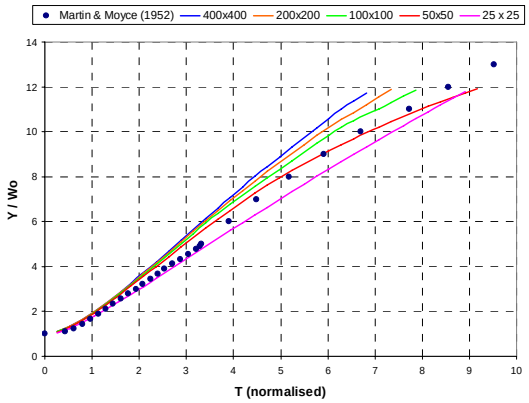

Fig. 8. *Comparison of surge front propagation using different total number of particles (np)*

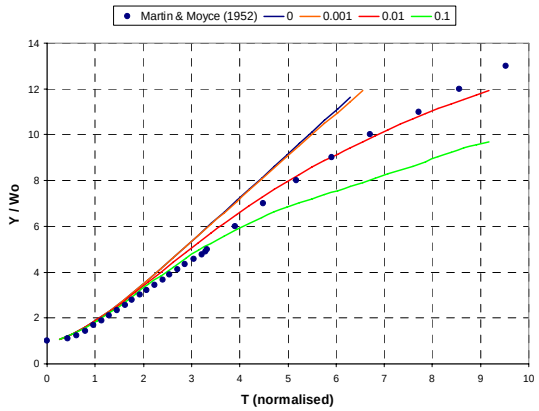

Fig. 9. *Comparison of surge front propagation using different wall viscosity coefficient (b)*

As seen in Figs. 8 and 9, the best agreement between measurements and simulations where a relatively low number of particles was used (np = 2500), was obtained using wall viscosity coefficient b = 0.01. When the same value of b and an increased number of particles were used however, the resulting propagation of surge front was too fast. This is particularly noticeable at larger distances from the upstream boundary, where the layer of fluid is thinner. One of the possible reasons for the faster propagation of the surge front could be the somewhat lower friction due to a thinner layer of particles contacting the rigid bottom and consequently, a larger number of particles travelling over such a boundary layer.

Therefore, the relation between wall viscosity coefficient (b) and the number of particles (np) which yields the best agreement between the observed and modelled surge front propagation, was studied further. Simulations using variable parameters np and b were performed in order to calibrate their interdependence. Fig. 10 shows the value of the coefficient b versus the number of particles at which the best agreement was achieved. Evidently, increasing the number of particles requires a simultaneous increase of the wall viscosity coefficient and the resulting ratio can

adequately be approximated by a linear relationship.

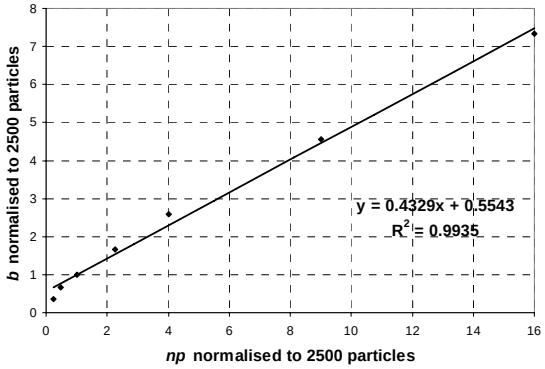

Fig. 10. *Correction coefficient for the wall viscosity coefficient b with different total number of particles np*

The new code is written in the C++ programming language and the input/output parameters and files are controlled by the Scilab open source platform. Compared to the SPHYSICS model, the new code runs more than 10-times faster for this case. Particularly with a higher total number of particles, this advantage of the new code can be highly significant.

3 CONCLUSIONS

We describe a new approach for boundary conditions for SPH simulations. This approach is based on continuous boundaries with friction and follows the derivation of the SPH equations with some reasonable simplifications. The new type of boundary condition presents a distinct improvement in comparison to the dynamic and repulsive boundary conditions used in similar models. Boundaries do not have to consist of particles, thus the total number of particles is lower. The disturbances of flow with no physical basis, which occur in the SPHYSICS model at the wall and at the surge front, are eliminated. The results of the new model are in good agreement with measurements. Particularly at larger normalised time, the results are in at least such a good agreement as those by other authors and better than the results of the SPHYSISC model. Moreover, in the simulated case, the new code was found to be much faster than the SPHYSICS model.

A sensitivity analysis showed the most important input parameters of the Tis Isat model. A new correction factor for wall viscosity with a different total number of particles was introduced in order to improve the agreement between the measured and simulated surge front propagation.

4 ACKNOWLEDGEMENT

The research was performed in the frame of the national project L2-0911 “Modelling of hydrodynamics, sediment transport and sediment bound pollutants using the SPH method” with a support of the Ministry of Higher Education, Science and Technology of the Republic of Slovenia (Programme P2-0180) and Soške Elektrarne Nova Gorica d.o.o.

5 REFERENCES

[1] Martin, J.C., Moyce, W.J. (1952). An experimental study of the collapse of liquid columns on a rigid horizontal plane. *Philos Trans Soc*, A 244, London, p. 312-324.

[2] Lucy, L.B. (1977). A numerical approach to the testing of the fission hypothesis. *Astron J,* vol. 82, no. 12, p. 1013-24.

[3] Gingold, R.A., Monaghan, J.J. (1977). Smoothed particle hydrodynamics. Theory and applicafion to non-spherical stars. Mon. Not, *Roy. Astron. Soc.,* vol. 181, p. 375-389.

[4] Libersky, L.D., Petsheck, A.G., Carney, T.C., Hipp, J.R., Allahdadi, F.A. (1993). High strain Lagrangian hydrodynamics - a three-dimensional SPH code for dynamic material response. *J. Comput. Phys.,* vol. 109, p. 67-75.

[5] Monaghan, J.J. (1994). Simulating free surface flows with SPH. *J. Comput. Phys.,* vol. 110, p. 399-406.

[6] Liu, M.B., Liu, G.R., Zong, Z., Lam, K.Y. (2003). Computer simulation of the high explosive explosion using smoothed particle hydrodynamics methodology. *Comput. Fluids,* vol. 32, no. 3, p. 305-322.

[7] Roubtsova, V., Kahawita, R. (2006). The SPH technique applies to free surface flows. *Computers & Fluids*, vol. 35, p. 1359-1371.

[8] Prakash, M., Debroux, F., Cleary, P. (2001). Three-dimensional modelling of dam break induced flows using Smooth Particle Hydrodynamics. *Proceedings of 14th*

Australian Fluid Mechanics Conference, Adelaide, p. 379-382.

[9] Gesteira, M.G., Rogers, B.D., Dalrymple, R.A., Crespo, A.J.C., Narayanaswamy, M. (2007). *User's guide to the SPHysics code*.

[10] Shao, S., Lo, E.Y.M. (2003). Incompressible SPH method for simulating Newtonian and non-Newtonian flows with a free surface. *Advances in Water Resources,* vol. 26, p. 787-800.

[11] Capone, T., Panizzo, A. (2008). SPH simulation of non-Newtonian mud flows. *Proc of SHPERIC III*., Lausanne, p. 134-137.

[12] Herault, A., Vicari, A., Del Negro, C.A. (2008). SPH thermal model for the cooling of a lava lake. *Proc of SHPERIC III.*, Lausanne, p. 143-148.

[13] Hu, X.Y., Adams, N.A. (2006). A multi-phase SPH method for macroscopic and mesoscopic flows. *Journal of Computational Physics,* vol. 213, p. 844-861.

[14] Colagrossi, A., Landrini, M. (2003). Numerical simulation of interfacial flows by smoothed particle hydrodynamics. *J. Comput. Phys.,* vol. 191, p. 448-475.

[15] Crespo, A.J.C., Gómez-Gesteira, M., Dalrymple, R.A. (2007). Boundary conditions generated by dynamic particles in SPH methods. CMC. *Computers, Materials, & Continua*, vol. 5, no. 3, p. 173-184.

[16] Randles, P.W., Libersky, L.D. (1996). Smoothed particle hydrodynamics: some recent improvements and applications. *Meth. Appl. Mech*. *Eng.*, vol. 139, no. 1-4, p. 375-408.

[17] Dalrymple, R.A., Knio, O. (2000). SPH modelling of water waves. *Proc. Coastal Dynamics*, Lund, p. 779-787.

[18] Marongiu, J.C., Leboef, F., Parkinson, E. (2007). A new treatment of solid boundaries. *Proc. of SHPERIC II.*, *Madrid*, p. 165-168.

[19] Monaghan J.J., Kos, A. (1999). Solitary waves on a Cretan beach. *J. Wtrwy. Port, Coastal and Ocean Engrg.,* vol. 125, p. 145-154.

[20] Kulasegaram, S., Bonet, J., Lewis, R.W., Profit, M. (2003). A variational formulation based contact algorithm for rigid boundaries in two-dimensional SPH applications. *Comput. Mech,* vol. 33, p. 316–325.

[21] Bonet, J., Rodriguez-Paz, M.X. (2005). Hamiltonian formulation of the variable-h SPH equations. *J. Comput. Phys*., vol. 209, p. 541–558.

[22] Monaghan, J.J. (1992). Smooth Particle Hydrodynamics. *Ann Rev Astron Astrophys,* Annual Reviews Inc., vol. 30, p. 573-574.

[23] Monaghan, J. J., Lattanzio, J. C. (1985). A refined particle method for astrophysical problems. *Astrophys.,* vol. 149, p. 135-143.

[24] Molteni, D., Colagrossi, A. (2008). Oblique impact of a jet on a plane surface solved by SPH: suggestions to improve the results of the pressure profiles. *Proc of SHPERIC III.*, Lausanne, p. 6-10.

[25] Verlet, L. (1967). Computer experiments on classical fluids: I. Thermodynamical properties of Lennard-Jones molecules. *Phys. Rev*, vol. 159, p. 98-103.

[26] SPHYSICS http://wiki.manchester.ac.uk/sphysics/index.php/Main_Page. Accessed 2010-07-05.

[27] Koshizuka, S., Oka, Y. (1996). Moving particle semi-implicit method for fragmentation of incompressible fluid. *Nuclear Science and Engineering,* vol. 123, p. 421-434.

[28] Jones, D.A., Belton, D. (2006). Smoothed particle hydrodynamics: applications within DSTO. *Defence Science and Technology Organisation, Victoria*, TR-1922, 47 p.

[29] Monaghan, J.J. (1989). On the problem of penetration in particle methods. *Journal Computational Physics,* vol. 82, p. 1-15.